DDX53 Regulates Cancer Stem Cell–Like Properties by Binding to SOX-2

Youngmi Kim, Minjeong Yeon, and Dooil Jeoung*

Department of Biochemistry, Kangwon National University, Chunchon 24341, Korea
*Correspondence: jeoungd@kangwon.ac.kr
http://dx.doi.org/10.14348/molcells.2017.0001
www.molcells.org

This study investigated the role of cancer/testis antigen DDX53 in regulating cancer stem cell-like properties. DDX53 shows co-expression with CD133, a marker for cancer stem cells. DDX53 directly regulates the SOX-2 expression in anti-cancer drug-resistant Malme3M[R] cells. DDX53 and miR-200b were found to be involved in the regulation of tumor spheroid forming potential of Malme3M and Malme3M[R] cells. Furthermore, the self-renewal activity and the tumorigenic potential of Malme3M[R]-CD133 (+) cells were also regulated by DDX53. A miR-200b inhibitor induced the direct regulation of SOX-2 by DDX53 We therefore, conclude that DDX53 may serve as an immunotherapeutic target for regulating cancer stem-like properties of melanomas.

Keywords: anti-cancer drug-resistance, cancer stem cell-like properties, DDX53, SOX-2

INTRODUCTION

Cancer /testis antigen DDX53 is found in the sera of various cancers (Cho et al., 2002; Iwata et al., 2005; Liggins et al., 2010). Methylation has an important role for the expression regulation of DDX53 (Cho et al., 2003). DDX53 regulates the expression of cyclins and acts as an oncogene (Por et al., 2010). DDX53 confers resistance to various anti-cancer drugs (Kim et al., 2010). miR-200b-DDX53 negative feedback loop (Kim et al., 2013) and miR-217-DDX53 feedback loop (Kim et al., 2016) regulate responses to anti-cancer drugs.

miRNAs are known to regulate cancer stem-cell like properties. miR-200b enhances sensitivity to erlotinib in lung cancer cells and cancer stem cell markers (Ahmad et al., 2013). miR-1181 negatively regulates the cancer stem cell-like properties in pancreatic cancer (Jiang et al., 2015). The downregulation of miRNA-148a, inhibits the stem cell-like properties of glioblastoma (Lopez-Bertoni et al., 2015). miR-200c negatively regulates the expression of SOX-2 to suppress PI3K-AKT pathway (Lu et al., 2014). miR-638 negatively regulates mesenchymal-like transition by directly targeting SOX-2 (Ma et al., 2014). By targeting OCT4/SOX-2 expression, the Lin28B-Let7 pathway regulates stemness properties of oral squamous cell carcinoma cells (Chien et al., 2015).

Cancer/testis antigens are overexpressed in cancer stem-like cells (Yang et al., 2015). MAGEA-3 is expressed in side population (SP) and main population (MP) cells derived from human bladder cancer SW780 cells (Yin et al., 2014). Since DDX53 regulates anti-cancer drug-resistance, the regulatory role of DDX53 in cancer stem cell-like properties has been further investigated.

In this study, we found that anti-cancer drug-resistant cancer cells have cancer stem cell-like properties. DDX53 showed a co-expression with CD133, and binding to SOX-2, a marker of cancer stemness. DDX53 directly regulated the expression of SOX-2 and the cancer stem cell-like properties in Malme3M[R] cells. We show a novel role of DDX53 in regulating cancer stem cell-like properties.

MAERIALS AND METHODS

Materials

Antibodies to MDR1, NANOG, YY1, PARP, SOX-2, and CAGE were purchased from Santa Cruz Biotechnology. Secondary antibodies conjugated to HRP and ECL kit (enhanced chemiluminescence) were purchased from Pierce Company. Lipofectamine and PlusTM reagent were purchased from Invitrogen. SiRNAs and miR-inhibitor were commercially synthesized by Bioneer Company (Korea).

Cell lines and cell culture

The melanoma cell lines (Malme3M, Malme3M^R) were grown in Dulbecco's Modified Eagle's Medium/Ham's Nutrient Mixture F-12 (DME/F12, Invitrogen). For all cell lines, media was supplemented with 10 % heat-inactivated fetal bovine serum (FBS, Invitrogen) and 1% penicillin/streptomycin (GIBCO). CD133$^+$ cells isolated from Malme3M^R, SNU387^R cells were maintained in serum-free DMEM/F12 (Gibco-BRL, USA) supplemented with 20 ng/ml epidermal growth factor (EGF) (Sigma, USA), 10 ng/ml basic fibroblast growth factor (bFGF) (Sigma, USA), and 20 ng/ml leukemia inhibitor factor (LIF) (Sigma, USA). Malme3M^R and SNU387^R cells were established from their parental Malme3M and SNU387 respectively by continuous exposure to celastrol (Kim et al., 2010). SNU387$^{R-AS-CAGE}$ and Mame3M$^{R-AS-CAGE}$ cells stably express anti-sense cDNA. Malme3M$^{R-miR-200b}$ cells stably express miR-200b (Kim et al., 2013).

Western blot and immunoprecipitation

Western blot and immunoprecipitation were performed as describe (Kim et al., 2014).

Chromatin immunoprecipitation (ChIP) Assays

The ChIP assay was performed using a ChIP assay kit (Upstate Biotechnology). Briefly, 2 × 10^6 cells were crosslinked with 1% (v/v) formaldehyde (Sigma) at 37℃ for 10 min and nuclear extracts were isolated. The nuclear lysates were immunoprecipitated with either anti-CAGE (1 μg/ml, Abcam), anti-SOX-2 (1 μg/ml, Santa Cruz) or rabbit IgG at 4℃ overnight. Purified immunoprecipitated DNAs were subjected to PCR. human SOX-2 promoter-1 [5'-TAAGGCTTTTG GCTA GGGC-3' (sense) and 5'-AAACTAACTGTGGCTGGCGA-3' (antisense)], SOX-2 promoter-2 [5'-TCTTGGTCTGCCCTTTGT GG-3' (sense) and 5'-TCCAATCAACCTTCCTGCCC-3' (antisense)], SOX-2 promoter-3 [5'-GGGCGGAGAGA GTGTTAC AG-3' (sense) and 5'-GCACTGTATGGAGGTGGC TT-3' (antisense)], SOX-2 promoter-4 [5'-GTGGGATGCCAGGAAGTT GA-3' (sense) and 5'-TT GTTCTCCCGCTCATCCAC-3' (antisense)] and SOX-2 promoter-5 [5'-AACTCCTGCACTG GCTG TTT-3' (sense) and 5'-TTTGTATCCCCTCTCGCAGC-3' (antisense)] were used to detect the binding of CAGE to the promoter sequences of SOX-2.

Transfection

The siRNA or control siRNA was purchased from Bioneer (Korea). To test the effect of miR-200b in Malme3M or Malme3M$^{R-miR-200b}$ cell lines, miR-200b inhibitor (Bioneer, Korea) was used to knockdown the expression of miR-200b.

The sequences used were 5'-UCAUCAUUACCCA GUAUUA-3' (miR-200b inhibitor) and 5'-GCAUAUAUCUA UUCCACUA-3' (control inhibitor).

RNA extraction and quantitative real-time PCR (qRT-PCR)

Total miRNA was isolated using the mirVana miRNA isolation kit (Ambion). miRNA was extended by a poly (A) tailing reaction using the A-Plus Poly (A) Polymerase Tailing Kit (Cell Script). CDNA was synthesized from miRNA with poly (A) tail using a poly (T) adaptor primer and qScript™ reverse transcriptase (Quanta Biogenesis). The expression level of miRNA gene was quantified with SYBR Green qRT-PCR kit (Ambion) using a miRNA-specific forward primer and a universal poly (T) adaptor reverse primer. For quantitative PCR, SYBR PCR Master Mix (Applied Biosystems) was used in a CFX96 Real-Time System thermocycler (BioRad).

Cell viability

Cell viability was determined by using the 3-(4, 5-dimethyl-thiazol-2-yl)-2, 5-diphenyltetrazolium bromide (MTT; Sigma).

Capsase-3 activity assays

Caspase-3 activity was measured according to the manufacturer's instructions (BioVision, USA).

Colony formation

Colonies were stained with 0.01% crystal violet and counted.

Flow cytometry

Briefly, 1 × 10^6 cells were incubated with 100 μl of 3 % BSA in PBS for 1 h on ice, then labeled with PE-conjugated anti-CD133 (Miltenyi Biotec, Germany), anti-CAGE (Abcam, Cambridge, UK) antibody bound to an Alexa-488 secondary antibody for 1 h. After washing three times with PBS, labeled cells were analyzed using flow cytometry using a FACSCalibur (BD Biosciences, USA)

Tumor spheroid formation assays

For tumor spheroid forming assay, CD133$^+$ and CD133$^-$ cells were plated (5 × 10^4 cells/well) in ultralow attachment plates (Corning Inc.) in DMEM/F12 stem cell medium. Cells were maintained at 37℃ in a humidified 5% CO$_2$ incubator and fed with 0.2 ml of fresh stem cell medium on days 2, 4 and 6. The total number of spheres was counted after 7 days by inverted microscopy (Olympus). To examine the self-renewal ability of CD133$^+$ and CD133$^-$ cells, primary spheres were dissociated with trypsin and 0.05% EDTA. Single cell suspension obtained from primary spheres were counted and re-plated in 6-well ultralow attachment plates. Secondary spheroids derived from single cells of primary spheres were examined by inverted microscopy (Olympus).

Immunofluorescence staining in spheroids

The expression of CAGE in spheroids formed from CD133$^+$ cells was analyzed by immunofluorescence staining. CD133$^+$ cells cultured in 24-well plates were fixed with 4% para-formaldehyde in PBS containing 0.2% Triton X-100 for 30 min at 4℃. After washing with PBS, incubated with 5% BSA in PBS for 1 h and then stained with primary anti-CAGE an-

tibody at 4℃ overnight. Spheroids were washed three times with PBS and incubated with secondary antibody Alexa-488-labeled goat anti-rabbit IgG for 1 h. Following the incubation, spheroids were washed three times with PBS and nuclei were stained with DAPI. Spheroids were observed under the fluorescence microscopy (Nikon TS 100, Nikon).

Immunohistochemistry staining
Paraffin-embedded tissue sections were immunostained using the Vecta stain ABC Elite Kit (Vector Laboratories). Tissue sections were deparaffinized with xylene and washed in ethanol. Endogenous peroxidase activity is blocked with 3% hydrogen peroxide and H_2O for 10 min. Slides were then blocked with 5% normal goat serum in TBS containing 0.1%Tween-20 (TBS-T) for 1 h. For immunohistochemistry staining, a primary antibody to DDX53 (1:100, Santa Cruz), MDR1 (1:100, Santa Cruz), SOX-2 (1:100, Santa Cruz) or IgG (1:100, Santa Cruz) was added and incubation continued at 4℃ for 24 h. After washing with TBS-T, incubation with biotinylated secondary antibody was continued for 30 min. After washing, slides were incubated in the ABC complex for 30 min, and then stained with diaminobenzidine (DAB, Sigma).

In vivo tumorigenic potential
Animal experiments were performed under an approved protocol by the Institutional Animal Care and Use Committee of Kangwon National University (KW-160329-2). All animals were housed in a laminar air-flow cabinet under aseptic conditions. To examine the tumorigenic potential of CD133^{+} cells, athymic nude mice (BALB/c nu/ nu, 5-6-week-old females) were used. Cells (1×10^6) were injected subcutaneously into the dorsal flank area of the mice. To test the effect of CAGE on *in vivo* tumorigenic potential, control siRNA (5 μM/kg) or CAGE siRNA (5 μM/kg) was injected intravenously after establishment of sizable tumor every three days for 20 days. At the end of experiments, all animals were sacrificed and tumors were removed. Tissues were fixed in 10% neutral-buffered formalin (Sigma, USA) and embedded in paraffin for histological studies or snap-frozen for protein analysis by Western blot. Also tumor fragments were subjected to isolate CD133^{+} and CD133^{-} cells using MACs system as described previously.

Isolation of CD133^{+} and CD133^{-} Cells
CD133^{+} and CD133^{-} Cells were isolated from Malme3M[R] cells by magnetic bead sorting using the MACs system (Miltenyi Biotec, Gladbach, Germany). For separation, cells were incubated with CD133 MicroBeads (100 μl/10^8 cells) for 30 min at 4℃ following treatment with FcR blocking reagent. For magnetic separation, cells were selected by MS columns (Miltenyi Biotec, Germany), which retained CD133^{+} cells linked by beads. Purity of isolated cells was evaluated by Western blotting. The fresh isolated CD133^{+} cells were cultured before assay in a stem cell medium containing serum-free DMEM/F12 medium (Gibco-BRL, USA), 20 ng/ml epidermal growth factor (EGF) (Sigma, USA), 10 ng/ml basic fibroblast growth factor (bFGF) (Sigma, USA), and 20 ng/ml leukemia inhibitor factor (LIF) (Sigma, USA). For isolation of CD133^{+} and CD133^{-} Cells from mouse xenograft, solid tissues were finely minced using sterile razor blades and forceps and incubated with dissociation buffer containing 200 units/ml of collagenase Type IV, 0.6 unit/ml of dispase and DNase I for 2 h at 37℃. Single cell suspension was obtained by filtering digested tissue through a 70 μm cell strainer and then gently loaded onto a layer of Ficoll-Paque gradient (Sigma) for separation of viable cells. After centrifugation at 500g for 30 min at room temperature, live nucleated cells were collected at the interface. Cell pellets were subjected to isolate CD133 (+) and CD133 (-) cells using MACs system as described above. The resulting cells were used as 1°CD133 (+) and 1°CD133 (-). 2°CD133 (+) and 2°CD133 (-) cells were obtained from xenograft tumor tissues formed by using 1°CD133 (+) cells.

Invasion and wound migration assay
Invasive potentials of CD133 (+) and CD133 (-) cells determined by using a transwell chamber system with 8-μm pore polycarbonate filter inserts (CoSTAR, Acton, MA). The lower and upper sides of the filter were coated with gelatin and matrigel (Sigma), respectively. The 1×10^4 cells in serum-free DME/F12 medium containing 0.1% BSA were plated into the upper chamber of an insert. A medium supplemented 10% FBS was added to the lower chamber. After incubation at 37℃ for 24 h, cells were fixed with methanol and the invaded cells were stained and counted. For wound healing migration assay, 2×10^5 cells were cultured as monolayer in a 24-well plate. Cells were scratched with 10-μl micropipette tip and washed three times with serum free medium. The cells were then placed in fresh serum-free medium at 37℃ for 48 h. Images of the scratch wounds were taken and measured by Image-Pro Plus software.

Statistical analysis
All data were analyzed by using the Student's *t*-test. The differences among the groups were considered statistically significance when p ⟨ 0.05.

RESULTS

DDX53 shows co-expression with CD133, a marker of cancer stemness
DDX53 increases level of cyclin D1 (Por et al., 2010), and induces anti-cancer drug-resistance (Kim et al., 2010). A close association has been suggested between anti-cancer drug-resistance and cancer stemness (Du et al., 2015). Therefore DDX53 may regulate cancer stem cell-like properties. We therefore examined whether DDX53 regulates cancer stem cell-like properties. Flow cytometry showed co-expression of DDX53 with CD133, a marker of cancer stemness in anti-cancer drug-resistant Malme3M[R] cells (Fig. 1A). Malme3M[R]-CD133 (+) and SNU387[R]-CD133 (+) cells showed higher level of DDX53, SOX-2, NANOG and MDR1 than Malme3M[R]-CD133 (-) and SNU387[R]-CD133 (-) cells (Fig. 1B). Immunofluorescence staining showed higher expression of DDX53 in Malme3M[R]-CD133 (+) cells than in Malme3M[R]-CD133 (-) cells (Fig. 1C). The downregulation of CD133 decreased the expression of SOX-2 and DDX53 in Malme3M[R]
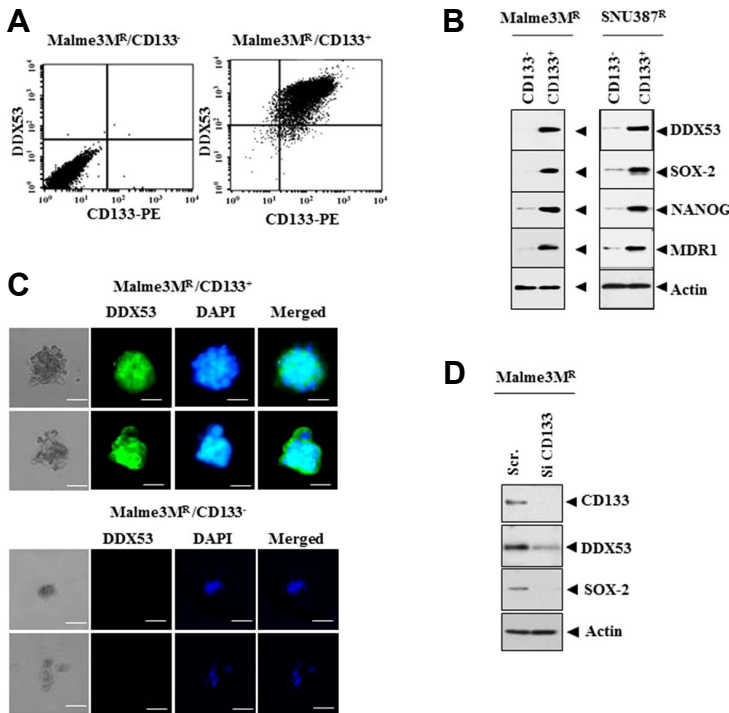
Fig. 1. DDX53 shows co-expression with CD133. (A) Malme3M[R]-CD133 (+) and Malme3M[R]-CD133 (-) cells were subjected to flow cytometry. (B) Western blot was performed. (C) Spheroids derived from Malme3M[R]-CD133 (+) cells or Malme3M[R]-CD133 (-) cells were subjected to immunofluorescence staining for expression analysis of DDX53. Scale bars represent 50 μm. (D) Malme3M[R] cells were transfected with the indicated siRNA (each at 10 nM). Western blot was performed after 48 h.
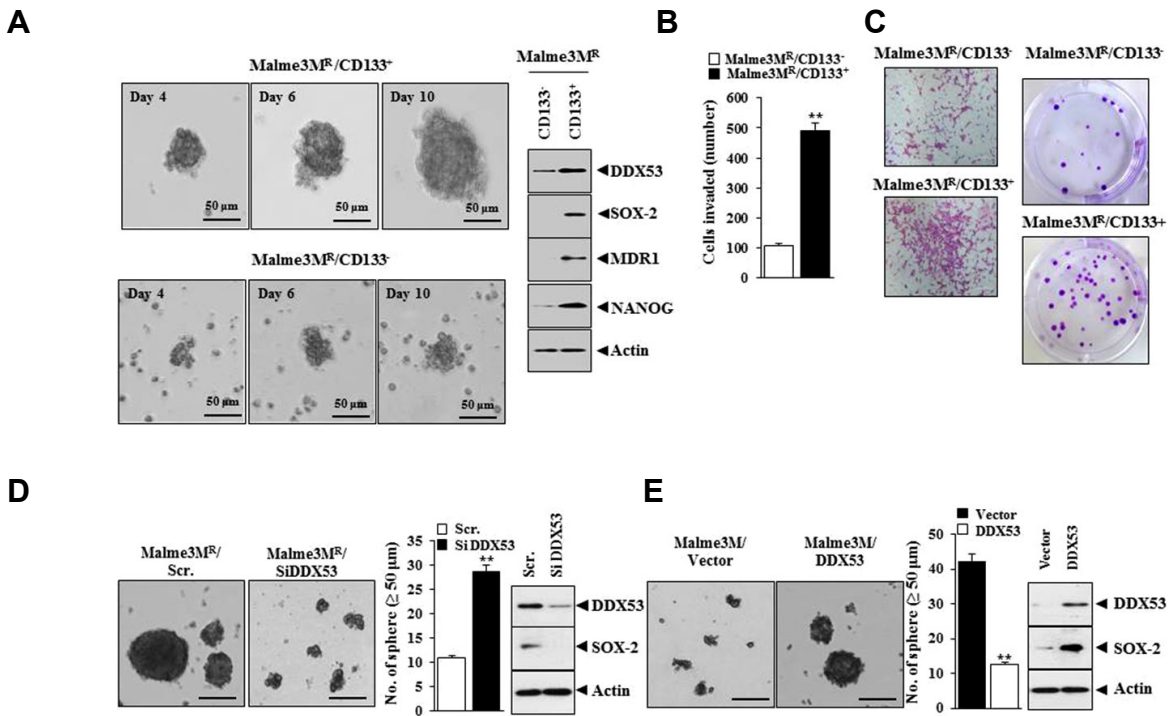

Fig. 2. DDX53 regulates the tumor spheroid forming potential of cancer cells. (A) Malme3M[R]-CD133 (+) and Malme3M[R]-CD133 (-) cells were subjected to tumor spheroid forming assays. Malme3M[R] cells were transfected with the indicated siRNA (each at 10 nM) for 48 h, followed by Western blot (right panel). ∗∗p < 0.005. (B) Chemoinvasion assays were performed. ∗∗p < 0.005. (C) Colony formation assays were performed. (D) At 48 h after transfection, Malme3M[R] cells were subjected to tumor spheroid formation assays and cell lysates were subjected to Western blot (right panel). ∗∗p < 0.005. Scale bars represent 50 μm. (E) At 48 h after transfection with the indicated construct (each at 1 μg), Malme3M cells were subjected to tumor spheroid formation assays and cell lysates were subjected to Western blot (right panel). ∗∗p < 0.005. Scale bars represent 50 μm.

cells (Fig. 1D). Taking these results into consideration, we believe that DDX53 may regulate cancer stem cell-like properties.

DDX53 regulates stem cell-like properties

Malme3M^R-CD133 (+) cells, but not Malme3M^R-CD133 (-) cells, show tumor spheroid forming potential (Fig. 2A). Malme3M^R-CD133 (+) cells showed higher expression of DDX53, SOX-2, NANOG and MDR1 (Fig. 2A), and greater invasion potential (Fig. 2B) than Malme3M^R- CD133 (-) cells. Malme3M^R-CD133 (+) cells showed higher growth potential than Malme3M^R- CD133 (-) cells based on colony formation assays (Fig. 2C). The decreased expression of DDX53 in Malme3M^R cells decreased the capacity of tumor spheroid formation, and the level of SOX-2 (Fig. 2D). DDX53 increased the tumor spheroid forming potential of Malme3M cells and the level of SOX-2 in Malme3M cells (Fig. 2E). Thus, we conclude that DDX53 regulates the stem cell-like properties of melanoma cells.

DDX53 binds to SOX-2 and directly regulates the expression of SOX-2

Next, we examined the role of DDX53 in regulating the expression of SOX-2. Malme3M^R and SNU387^R cells display higher level of DDX53, SOX-2 and NANOG, than the Malme3M and SNU387 cells (Fig. 3A). Malme3M$^{R-As-DDX53}$ and SNU387 $^{R-As-DDX53}$ cells stably expressing the anti-sense DDX53 displayed lower level of DDX53, SOX-2 and NANOG, than

Malme3M^R and SNU387^R cells (Fig. 3B). The SOX-2 promoter sequences contain binding sites for HDAC2, YY1, SOX9, AP4 and Elk-1 (Fig. 3C). DDX53 interacts with HDAC2 (Kim et al., 2010), and Hdac1/2 deficiency decreases SOX-2 level, thereby blocking the proximal airway development (Wang et al., 2013). Hence, we examined if DDX53 binds to the promoter sequences of SOX-2. DDX53 and YY1 showed binding to the promoter sequences of SOX-2 (Fig. 3C). DDX53 showed an interaction with SOX-2 in Malme3M^R cells and the decreased expression of SOX-2 decreased the level of DDX53 in Malme3M^R cells (Fig. 3D). Thus DDX53, through interaction with SOX-2, regulates the cancer stem cell-like properties.

The decreased expression of SOX-2 enhances sensitivity to anti-cancer drugs

The downregulation of NANOG enhances the inhibitory effects of resveratrol on self-renewal capacity of cancer stem cells (Shankar et al., 2011). Gefitinib resistance results from high expression of cancer stem cells markers such as CD133, SOX-2 and NANOG (Murakami et al., 2014). Taxol increases the level of DDX53, SOX-2 and NANOG in Malme3M cells (Fig. 4A). The decreased expression of SOX-2 induces cleavage of PARP (Fig. 4B), enhanced sensitivity (Fig. 4C) and capsase-3 activity (Fig. 4D) in response to taxol in Malme3M^R cells. The downregulation of SOX-2 decreased the invasion and migration potential, whereas DDX53 restored the invasion and migration potential of Malme3M^R cells transfected with SiSOX-2 (Fig. 4E).
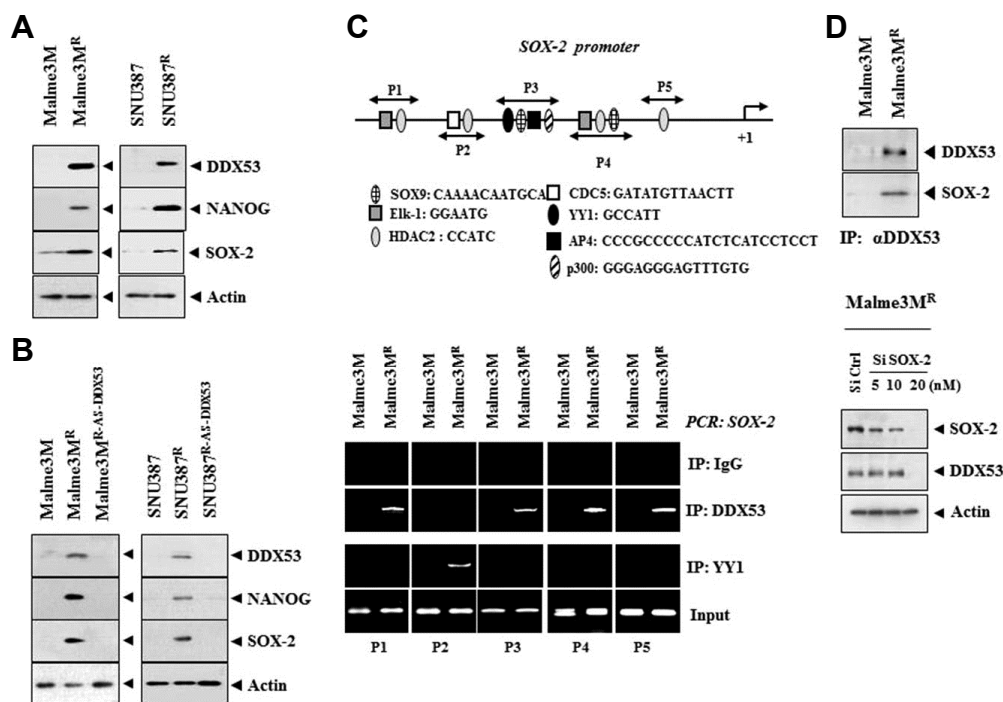

Fig. 3. DDX53 interacts with SOX-2, and directly regulates the expression of SOX-2. (A, B) Cell lysates from the indicated cancer cells were subjected to Western blot. (C) Cell lysates isolated from the indicated cancer cells were subjected to ChIP assays. (D) Cell lysates from the indicated cancer cells were subjected to immunoprecipitation, followed by Western blot (upper panel). At 48 h after transfection with the indicated siRNA, cell lysates were subjected to Western blot (right panel).
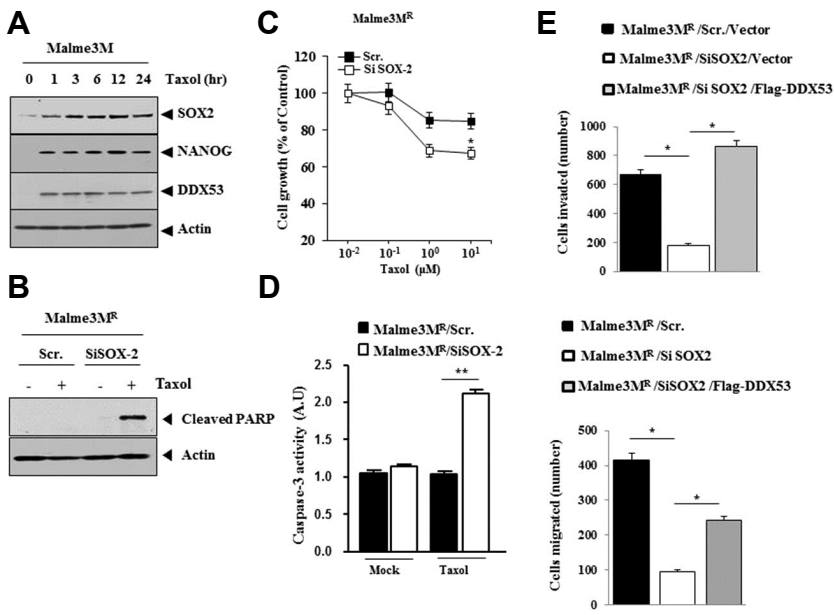
Fig. 4. The decreased expression of SOX-2 confers anti-cancer drug-sensitivity. (A) Malme3M cells were treated with taxol (1 μM). Cell lysates prepared at each time point were subjected to Western blot. (B) At 24 h after transfection with the indicated siRNA (each at 10 nM), Malme3M^R cells were treated with taxol (1 μM) for 24 h, followed by Western blot. (C) At 24 h after transfection with the indicated siRNA (each at 10 nM), Malme3M^R cells were treated with various concentrations of taxol for 24 h, followed by MTT assays. *$p <$ 0.05. (D) At 24 h after transfection with the indicated siRNA (each at 10 nM), Malme3M^R cells were treated with taxol (1 μM) for 24 h, followed by caspase-3 activity assays. **$p <$ 0.005. (E) After transfection with indicated siRNA (each at 10 nM) along with the indicted construct (each at 1 μg), Malme3M^R cells were subjected to chemoinvasion and migration assays. *$p <$ 0.05.
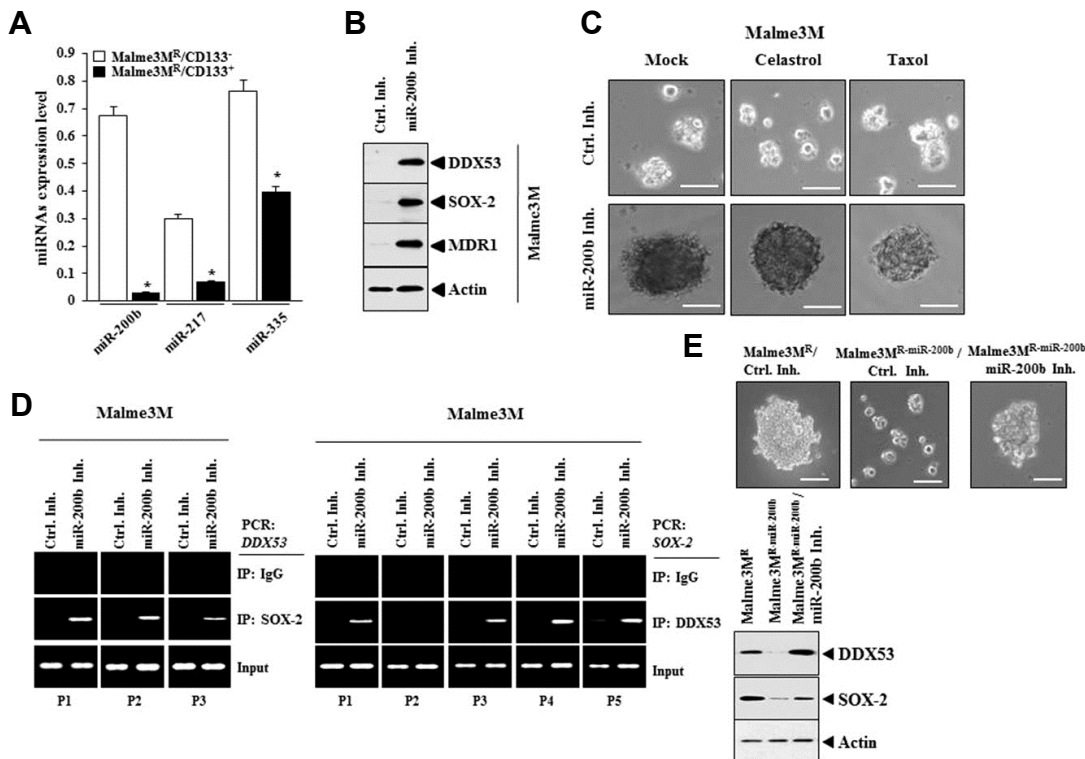

Fig. 5. miR-200b, a negative regulator of DDX53, regulates the cancer stem cell-like properties. (A) The level of the indicated miRNAs from Malme3M^R-CD133 (+) and Malme3M^R -CD133 (-) cells was determined by qRT-PCR. *$p <$ 0.05. (B) At 48 h after transfection with the indicated inhibitor (each at 10 nM), Western blot was performed. (C) At 24 h after transfection with the indicated inhibitor (each at 10 nM), Malme3M cells were treated with celastrol (1 μM) or taxol (1 μM). Tumor spheroid formation assays were performed. (D) At 48 h after transfection with the indicated inhibitor (each at 10 nM), ChIP assays employing the indicated antibody (2 μg/ml) were performed. (E) The indicated cancer cells were transfected with the indicated inhibitor (each at 10 nM), followed by tumor spheroid formation assays (upper panel) and Western blot (lower panel).

miR-200b inhibitor increases the level of SOX-2, induces an interaction between DDX53 and SOX-2 and regulates the tumor spheroid forming potential

miR-200b (Kim et al., 2013) and miR-217 (Kim et al., 2016) decrease the level of DDX53. The levels of miR-200b, miR-217 and miR-335 were lower in Malme3M[R]-CD133 (+) cells than in Malme3M[R]-CD133 (-) cells (Fig. 5A). Exposure to miR-200b inhibitor increased the level of DDX53, SOX-2, MDR1 (Fig. 5B) and tumor spheroid forming potential of Malme3M cells, regardless of the presence of celastrol and taxol (Fig. 5C). The miR-200b inhibitor induces the binding of SOX-2 to the promoter sequences of DDX53 (Fig. 5D), whereas the miR-200b induced the binding of DDX53 to the promoter sequences of SOX-2 (Fig. 5D). The miR-200b inhibitor enhances the tumor spheroid forming potential of Malme3M[R-miR-200b] cells (Fig. 5E), and restores the expression of DDX53 and SOX-2 Malme3M[R-miR-200b] cells (Fig. 5E). Thus, DDX53 regulates cancer stem cell-like properties.

DDX53 regulates tumorigenic potential of Malme3M[R]-CD133 (+) cells

Pancreatic cancer stem cells (CD133 (+) CD44 (+) CD24 (+) ESA (+)) show tumorigenic potential in NOD/SCID mice (Shankar et al., 2011). The downregulation of DDX53 decreases the tumorigenic potential of Malme3M[R]-CD133 (+) cells (Fig. 6A). Immunohistochemistry staining showed the decreased expression of SOX-2 and MDR1 by downregulation of DDX53 (Fig. 6B). The downregulation of DDX53 also decreased the levels of CD133, SOX-2, MDR1 and the interaction between DDX53 and SOX-2 (Fig. 6C). Thus, DDX53 regulates the tumorigenic potential of cancer stem cells.

DDX53 regulates self-renewal of CD133 (+) cells

Because DDX53 regulated the tumor spheroid forming potential of cancer cells (Figs. 2D and 2E), we examined whether DDX53 affects the self- renewal of cancer stem cells. 1° xh CD133 (+) cells, isolated from xenograft of Malme3M[R] cells (Fig. 7A), display higher tumor spheroid forming poten-

tial than 1° xh CD133 (-) cells in the absence and presence of anti-cancer drugs (Fig. 7B). 1° xh CD133 (+) cells displayed higher expression of DDX53, SOX-2 and MDR1 than 1° xhCD133 (-) cells (Fig. 7C). 2° xhCD133 (+) cells, isolated from the xenograft of Malme3M[R]-CD133 (+) cells (Fig. 7A), also showed higher tumor spheroid forming potential than 2° xhCD133 (-) cells in the absence and presence of anti-cancer drugs (Fig. 7D), and higher expression of DDX53 and SOX-2 than 2° xhCD133 (-) cells (Fig. 7E). These results suggest that DDX53 regulates the self-renewal capacity of Malme3M[R]-CD133 (+) cells.

DISCUSSION

DDX53 showed co-expression with CD133 in Malme3M[R] cells (Fig. 1A). Malme3M[R]-CD133 (+) cells have higher levels of DDX53, SOX-2 and NANOG than Malme3M[R]-CD133 (-) cells (Fig. 1B). These results suggest the involvement of DDX53 in regulating cancer stem cell-like properties. Given the fact that Malme3M[R]-CD133 (+) cells express higher expression of MDR1 than Malme3M[R]-CD133 (-) cells (Fig. 1B), it is probable that cancer stemness is related to anti-cancer drug resistance.

We found an interaction between DDX53 with SOX-2 in Malme3M[R] cells (Fig. 3D). SOX-2 interacts with HDAC2 (Cox et al., 2010). DDX53 interacts with HDAC2 (Kim et al., 2010). It is therefore reasonable that DDX53 interacts with HDAC2 to regulate the expression of SOX-2.

HDAC3 confers sensitivity to anti-cancer drugs (Kim et al., 2014), decreases the level of MDR1 (Park et al., 2014b) and reduces angiogenic potential (Park et al., 2014a). Thus HDAC3 may negatively regulate cancer stem cell-like properties. miR-326 forms a negative feedback loop with HDAC3 and induces anti-cancer drug-resistance (Kim et al., 2014). Thus miR-326 may positively regulate the cancer stem cell-like properties of Malme3M[R] cells. miR-335 increases the level of HDAC3 by targeting SIAH2 (Kim et al., 2015). Thus, SIAH2 may thereby regulate cancer stem cell-like properties.
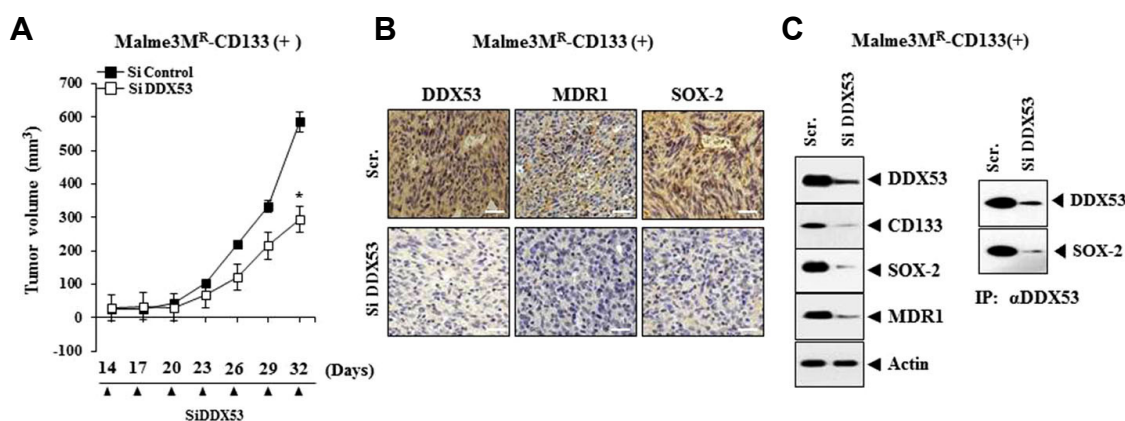

Fig. 6. DDX53 regulates the tumorigenic potential of Malme3M[R]-CD133 (+) cells. (A) Malme3M[R]-CD133(+) cells (10[6] cells) were subcutaneously injected into athymic nude mice. The indicated siRNA (50 μM/kg) was intravenously injected 7 times over a period of 32 days. The extent of tumorigenic potential was determined. *p < 0.05. (B) Immunohistochemistry staining employing tumor tissue was performed, as described. (C) Immunoprecipitation and Western blot employing tumor tissue lysates were performed.
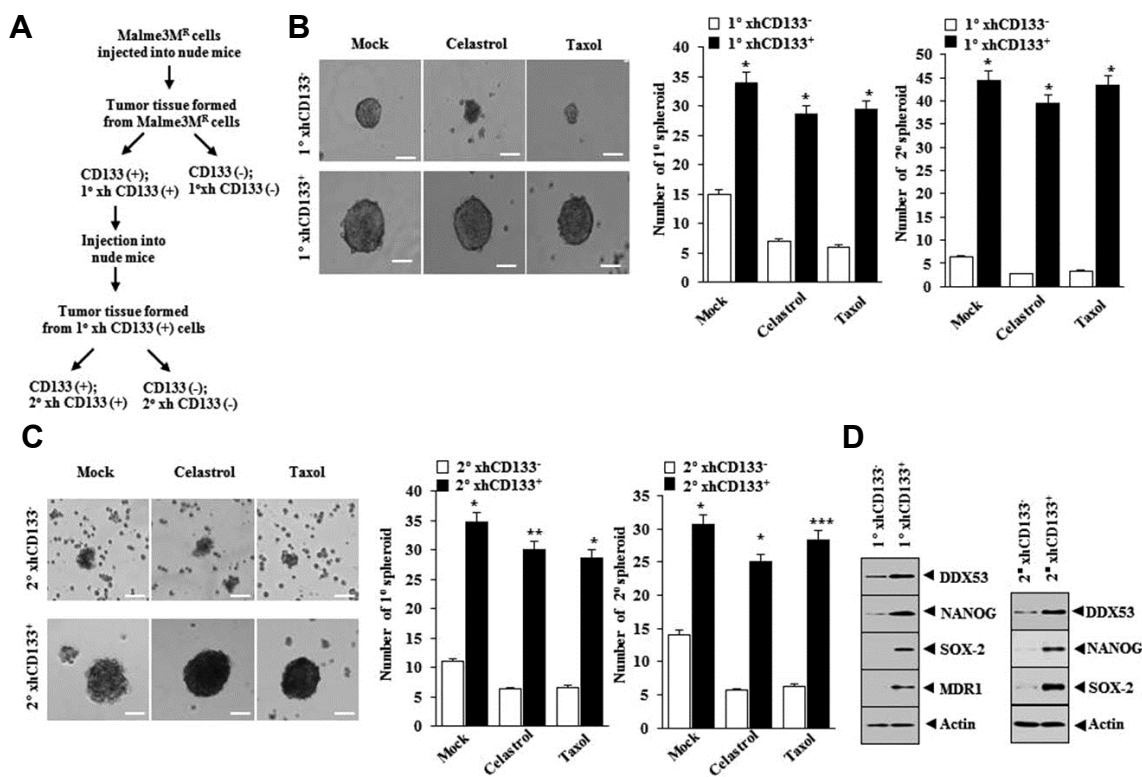
Fig. 7. Malme3M^R-CD133 (+) cells shows self-renewal capacity. (A) 1° xhCD133 (+) and 1° xhCD133 (-) cells were from tumor tissues formed from Malme3M^R cells. 2° xhCD133 (+) and 2° xhCD133 (-) cells were from tumor tissues formed from 1° xhCD133 (+) cells injected into nude mice. (B) 1° xhCD133 (+) and 1° xhCD133 (-) cells were subjected to tumor spheroid formation assays in the absence or presence of celastrol (1 μM) or taxol (1 μM). Primary spheroids obtained from 1° xhCD133 (+) or 1° xhCD133 (-) cells were dissociated to yield single cell suspension. Thus obtained single suspension was subjected to tumor spheroid formation to obtain secondary tumor spheroids. *p < 0.05. (C) 2° xhCD133 (+) and 2° xhCD133 (-) cells were subjected to tumor spheroid formation assays. Primary spheroids obtained from 2° xhCD133 (+) or 2° xhCD133 (-) cells were dissociated to yield single cell suspension. Thus obtained single suspension was subjected to tumor spheroid formation to obtain secondary tumor spheroids. *p < 0.05; **p < 0.005; ***p < 0.0005. (D) Western blot was performed.

Autophagy is involved in the regulating the levels of OCT4, NANOG and SOX-2 (Cho et al., 2014). Autophagy inhibition enhances the chemotherapeutic effects of gemcitabine, mitomycin and cisplatin (Ohja et al., 2014). Compared to Malme3M cells, the Malme3M^R cells show a higher expression of LC3-I/II, a marker of autophagy, while showing lower expression of p62, an inhibitor of autophagy (data not shown). Therefore, anti-cancer drug-resistance is closely related with autophagy.

miRNAs are critical for cancer stemness. miR-145-5p reduces the tumorigenic potential of cancer cells and the level of SOX-2 (Ozen et al., 2015). miR-29b negatively regulates stemness maintenance in glioblasotoma multiforme by attenuating tube formation and the expression of VEGF and Ang-2 (Chung et al., 2015). TargetScan analysis predicts that ATG-5,-7, and -12 serve as targets of miR-200b and miR-217. DDX53 regulates the expression of various autophagy marker proteins, such as p62, pBeclin^{Ser15}, ad LC3I/II (Personal observations). Over-expression of DDX53 enhances autophagy (Personal observations). These results suggest that DDX53 regulates cancer stemness in association with its effect on autophagy. The effect of marker proteins of autophagy, such as p62, pBeclin^{Ser15}, and LC3I/II, on the cancer stemness of Malme3M^R cells would merit investigation.

In this study, we present the mechanism of cancer stemness regulated by DDX53. Thus, we propose that DDX53 may serve as a target for the development of anti-cancer therapies.

REFERENCES

Ahmad, A., Maitah, M.Y., Ginnebaugh, K.R., Li, Y., Bao, B., Gadgeel, S.M., and Sarkar, F.H. (2013). Inhibition of Hedgehog signaling sensitizes NSCLC cells to standard therapies through modulation of

EMT-regulating miRNAs. J. Hematol. Oncol. 6, 77.

Chien, C.S., Wang, M.L., Chu, P.Y., Chang, Y.L., Liu, W.H., Yu, C.C., Lan, Y.T., Huang, P.I., Lee, Y.Y., Chen, Y.W., et al. (2015). Lin28B/Let-7 regulates expression of Oct4 and Sox2 and reprograms oral squamous cell carcinoma cells to a stem-like state. Cancer Res. 75, 2553-2565.

Cho, B., Lim, Y., Lee, D.Y., Park, S.Y., Lee, H., Kim, W.H., Yang, H., Bang, Y.J., and Jeoung, D.I. (2002). Identification and characterization of a novel cancer/testis antigen gene CAGE. Biochem. Biophys. Res. Commun. 292, 715-726.

Cho, B., Lee, H., Jeong, S., Bang, Y.J., Lee, H.J., Hwang, K.S., Kim, H.Y., Lee, Y.S., Kang, G.H., and Jeoung, D.I. (2003). Promoter hypomethylation of a novel cancer/testis antigen gene CAGE is correlated with its aberrant expression and is seen in premalignant stage of gastric carcinoma. Biochem. Biophys. Res. Commun. 307, 52-63.

Cho, Y.H., Han, K.M., Kim, D., Lee, J., Lee, S.H., Choi, K.W., Kim, J., and Han, Y.M. (2014). Autophagy regulates homeostasis of pluripotency-associated proteins in hESCs. Stem Cells 32, 424-435.

Chung, H.J., Choi, Y.E., Kim, E.S., Han, Y.H., Park, M.J., and Bae, I.H. (2015). miR-29b attenuates tumorigenicity and stemness maintenance in human glioblastoma multiforme by directly targeting BCL2L2. Oncotarget 6, 18429-18444.

Cox, J.L., Mallanna, S.K., Luo, X., and Rizzino, A. (2010). Sox2 uses multiple domains to associate with proteins present in Sox2-protein complexes. PLoS One 5, e15486.

Du, J., Liu, S., He, J., Liu, X., Qu, Y., Yan, W., Fan, J., Li, R., Xi, H., Fu, W., et al. (2015). MicroRNA-451 regulates stemness of side population cells via PI3K/Akt/mTOR signaling pathway in multiple myeloma. Oncotarget 6, 14993-15007.

Iwata, T., Fujita, T., Hirao, N., Matsuzaki, Y., Okada, T., Mochimaru, H., Susumu, N., Matsumoto, E., Sugano, K., Yamashita, N., Nozawa, S., and Kawakami, Y. (2005). Frequent immune responses to a cancer/testis antigen, CAGE, in patients with microsatellite instability-positive endometrial cancer. Clin. Cancer Res. 11, 3949-3957.

Jiang, J., Li, Z., Yu, C., Chen, M., Tian, S., and Sun, C. (2015). MiR-1181 inhibits stem cell-like phenotypes and suppresses SOX2 and STAT3 in human pancreatic cancer. Cancer Lett. 356, 962-970.

Kim, Y., Park, H., Park, D., Lee, Y.S., Choe, J., Hahn, J.H., Lee, H., Kim, Y.M., and Jeoung, D. (2010). Cancer/testis antigen CAGE exerts negative regulation on p53 expression through HDAC2 and confers resistance to anti-cancer drugs. J. Biol. Chem. 285, 25957-25968.

Kim, Y., Park, D., Kim, H., Choi, M., Lee, H., Lee, Y.S., Choe, J., Kim, Y.M., and Jeoung, D. (2013). miR-200b and cancer/testis antigen CAGE form a feedback loop to regulate the invasion and tumorigenic and angiogenic responses of a cancer cell line to microtubule-targeting drugs. J. Biol. Chem. 288, 36502-36518.

Kim, Y., Kim, H., Park, H., Park, D., Lee, H., Lee, Y.S., Choe, J., Kim, Y.M., and Jeoung, D. (2014). miR-326-histone deacetylase-3 feedback loop regulates the invasion and tumorigenic and angiogenic response to anti-cancer drugs. J. Biol. Chem. 289, 28019-28039.

Kim, Y., Kim, H., Park, D., and Jeoung, D. (2015). miR-335 Targets SIAH2 and confers sensitivity to anti-cancer drugs by increasing the expression of HDAC3. Mol. Cells 38, 562-572.

Kim, Y., Kim, H., Park, D., Han, M., Lee, H., Lee, Y.S., Choe, J., Kim, Y.M., and Jeoung, D. (2016). miR-217 and CAGE form feedback loop and regulates the response to anti-cancer drugs through EGFR and HER2. Oncotarget 7, 10297-10321.

Liggins, A.P., Lim, S.H., Soilleux, E.J., Pulford, K., and Banham, A.H. (2010). A panel of cancer-testis genes exhibiting broad-spectrum expression in haematological malignancies. Cancer Immun. 10, 8.

Lopez-Bertoni, H., Lal, B., Li, A., Caplan, M., Guerrero-Cázares, H., Eberhart, C.G., Quiñones-Hinojosa, A., Glas, M., Scheffler, B., Laterra, J., and Li, Y. (2015). DNMT-dependent suppression of microRNA regulates the induction of GBM tumor-propagating phenotype by Oct4 and Sox2. Oncogene 34, 3994-4004.

Lu, Y.X., Yuan, L., Xue, X.L., Zhou, M., Liu, Y., Zhang, C., Li, J.P., Zheng, L., Hong, M., and Li, X.N. (2014). Regulation of colorectal carcinoma stemness, growth, and metastasis by an miR-200c-Sox2-negative feedback loop mechanism. Clin. Cancer Res. 20, 2631-2642.

Ma, K., Pan, X., Fan, P., He, Y., Gu, J., Wang, W., Zhang, T., Li, Z., and Luo, X. (2014). Loss of miR-638 in vitro promotes cell invasion and a mesenchymal-like transition by influencing SOX2 expression in colorectal carcinoma cells. Mol. Cancer 13, 118.

Murakami, A., Takahashi, F., Nurwidya, F., Kobayashi, I., Minakata, K., Hashimoto, M., Nara, T., Kato, M., Tajima, K., Shimada, N., et al. (2014). Hypoxia increases gefitinib-resistant lung cancer stem cells through the activation of insulin-like growth factor 1 receptor. PLoS One 9, e86459.

Ojha, R., Jha, V., Singh, S.K., and Bhattacharyya, S. (2014). Autophagy inhibition suppresses the tumorigenic potential of cancer stem cell enriched side population in bladder cancer. Biochim. Biophys. Acta. 1842, 2073-2086.

Ozen, M., Karatas, O.F., Gulluoglu, S., Bayrak, O.F., Sevli, S., Guzel, E., Ekici, I.D., Caskurlu, T., Solak, M., Creighton, C.J., et al. (2015). Overexpression of miR-145-5p inhibits proliferation of prostate cancer cells and reduces SOX2 expression. Cancer Invest. 33, 251-258.

Park, D., Park, H., Kim, Y., Kim, H., and Jeoung, D. (2014a). HDAC3 acts as a negative regulator of angiogenesis. BMB Rep. 47, 227-232.

Park, H., Kim, Y., Park, D., and Jeoung, D. (2014b). Nuclear localization signal domain of HDAC3 is necessary and sufficient for the expression regulation of MDR1. BMB Rep. 47, 342-347.

Por, E., Byun, H.J., Lee, E.J., Lim, J.H., Jung, S.Y., Park, I., Kim, Y.M., Jeoung, D.I., and Lee, H. (2010). The cancer/testis antigen CAGE with oncogenic potential stimulates cell proliferation by up-regulating cyclins D1 and E in an AP-1- and E2F-dependent manner. J. Biol. Chem. 285, 14475-14485.

Shankar, S., Nall, D., Tang, S.N., Meeker, D., Passarini, J., Sharma, J., and Srivastava, R.K. (2011). Resveratrol inhibits pancreatic cancer stem cell characteristics in human and KrasG12D transgenic mice by inhibiting pluripotency maintaining factors and epithelial-mesenchymal transition. PLoS One 6, e16530.

Wang, Y., Tian, Y., Morley, M.P., Lu, M.M., Demayo, F.J., Olson, E.N., and Morrisey, E.E. (2013). Development and regeneration of Sox2+ endoderm progenitors are regulated by a Hdac1/2-Bmp4/Rb1 regulatory pathway. Dev. Cell 24, 345-358.

Yang, P., Huo, Z., Liao, H., and Zhou, Q. (2015). Cancer/testis antigens trigger epithelial-mesenchymal transition and genesis of cancer stem-like cells. Curr. Pharm. Des. 21, 1292-1300.

Yin, B., Zeng, Y., Liu, G., Wang, X., Wang, P., and Song, Y. (2014). MAGE-A3 is highly expressed in a cancer stem cell-like side population of bladder cancer cells. Int. J. Clin. Exp. Pathol. 7, 2934-2941.